

STRAIN DRIVEN CHANGES OF DEFECT PARAMETERS IN HEAVY ION IMPLANTED Si

C. PALADE^a, A.M. LEPADATU^a, A. SLAV^a, M. L. CIUREA^{a,b}, S. LAZANU^{a,*}

^aNational Institute of Materials Physics, 105 bis Atomistilor Street, Magurele
077125, Romania

^bAcademy of Romanian Scientists, 54 Splaiul Independentei, Bucharest 050094
Romania

We analyse the influence of the strain field on the parameters of trapping centres. The system under study is high resistivity Si implanted with Bi⁶⁺ and I⁶⁺ ions respectively, of 28 MeV kinetic energy, 3° off <100> axis orientation and 5x10¹¹ ions/cm² fluence. The strain field is the consequence of size and mass difference of the irradiation ions in respect to the atoms of the lattice, and the defects are produced during the slowing-down of ions, as a result of the energy transfer from the ion to Si atoms. These results are of interest for the design and manufacturing of microelectronic devices incorporating strain, particularly for quantum computers with qubits based on the interaction of electronic and nuclear spins of group-V donors in Si.

(Received October 20, 2015; Accepted December 2, 2015)

Keywords: Ion irradiation defects; Trapping centres; Field of strain

1. Introduction

Strain engineering represents a modern field of research, and in spite of the fact that the interest for the strain field and its effects on semiconductors dates more than sixty years before, starting with the pioneering studies of Bardeen and Shockley related to the coupling of acoustic phonons and electrons, there are a lot of open problems. Strain engineering aims to boost performance, in conditions of scaling limitations for devices. So, by using strain, an enhancement of the performances of different electronic devices was obtained without increasing the processing complexity [1]. Strain affects the physical, electronic, optical and magnetic properties of crystals, and it is introduced either across the entire substrate in global strain techniques or locally in selected regions of the wafer [2, 3]. Examples of devices incorporating strain cover piezoresistive strain sensors [4], quantum well lasers with lattice-mismatched heterostructures [5], magnetomechanical actuators based on Ni-Mn-Ga alloys and on Ni/PZT [6, 7], strain enhanced MOSFETs as FinFET [8, 9] and superjunction VDMOS [10], but also those using high atomic mass and size dopants, (*e.g.* those to be used in quantum computing and quantum sensing due to their very high coherence times [11]), up to “straintronic” devices [12]. New techniques are simultaneously developed to measure the strain through the thickness of a crystal [13], or to demonstrate the presence of extremely low amounts of strain in thin semiconductor epilayers [14].

The present paper tackles the topic of strain field from the point of view of defects, the presence and behaviour of which dictate the performance of semiconductor devices. The strain is produced simultaneously with irradiation defects, by implanting I and Bi ions of 28 MeV kinetic energy into high resistivity Si. Both ions have higher atomic size and mass in respect to Si atoms, and consequently produce a local deformation of the lattice. In order to devise the influence of strain on the trapping characteristics of defects, the information obtained from the simulation of the penetration of ions in silicon, *i.e.* distributions of stopped ions and primary defects, is

* Corresponding author: lazanu@infim.ro

integrated with the results obtained from modelling experimental measurements (parameters of the trapping centres). The differences found in the characteristics of the trapping centres corresponding to Bi and I implanted Si samples are put in relation and explained based on the fields of strain created by the two ions.

2. Heavy ion penetration into Si

High resistivity Si wafers, (100) oriented and of 280 μm thickness, produced by Siltronic, were irradiated with Bi and I ions of 28 MeV kinetic energy and 5×10^{11} ions/cm² fluence at the Uppsala tandem accelerator. The beam line was 3° disoriented in respect to (100) Si axis, and the radiation non-uniformity on wafer surface was less than 5%.

The incoming ions are eventually stopped in the sample, as a consequence of losing their kinetic energy by interaction with ions and electrons of the host lattice. The mechanisms of energy loss are classified in nuclear and electronic collisions. In the first case, the ions transfer energy to the translatory motion of an atom as a whole, while in the second case the energy is transmitted to target electrons, which are excited or ejected from atoms. Nuclear collisions can involve large discrete energy transfers and also large deflection angles, and are responsible for defect production in the lattice. Displacement damage is based on the creation of cascades of displacements following the interaction of an incoming energetic ion with an atom placed in its site. If the energy transmitted in the collision surpasses the threshold for displacements, the atom becomes a self-recoil and leaves behind a vacancy. In its turn the self-interstitial moves through the lattice and interacts similarly with other atoms, and the process continues up to the moment the energy transmitted in a collision is lower than the threshold for displacements.

We have simulated the penetration of both Bi and I ions into Si, using the Monte Carlo code *Stopping and Range of Ions in Matter* (SRIM), based on the binary collision approximation. The program follows the slowing-down of the primary particle and of all particles set in motion by it, until they either leave the target or fall below a selected low kinetic energy. In each case, 2000 ions were simulated, in order to find the positions of the stopped ions and the distributions of vacancies created. In the SRIM computer code, the sample is considered to be amorphous. The results are then compared with those obtained using a computer code with keeps into account the crystalline structure of the sample, for different orientations of the beam in respect to the crystal axes.

2.1 Distribution of stopped ions

The heavy ions stopped in the lattice, being bigger and heavier than Si ones, produce a local strain [15, 16], which is strongly dependent on their positions. This is the reason the location of the stopped ions is of high interest in the present study. In Figs. 1 and 2 we present the 3D profile of stopped ions, their positions in the depth-radius plane, and also the 2D profiles of the ions in the depth of the sample, for Bi and I respectively. The distribution of stopped ions in the depth is a Pearson distribution, which in both cases is a nearly Gaussian one with a small tail toward the surface.

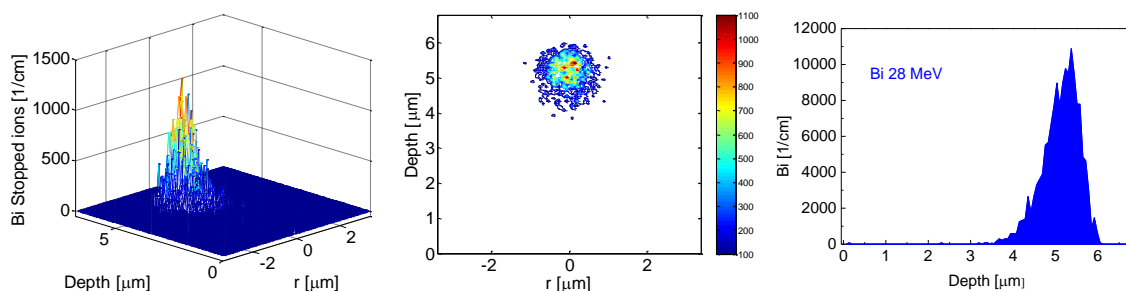


Fig. 1 Distribution of stopped Bi ions: a) 3D profile; b) position in depth-radius plane; c) depth distribution

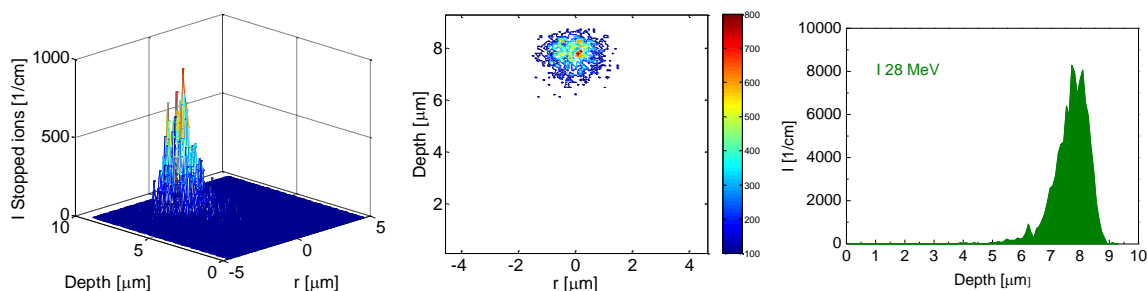


Fig. 2 Distribution of stopped I ions: a) 3D profile; b) position in depth-radius plane; c) depth distribution

From this simulation, we obtain for the average (projected) range and range straggling (longitudinal standard deviation) the values of 5.09 and 0.42 μm for Bi, and 7.65 and 0.55 μm for I respectively. The corresponding mean radial ranges are 0.49 and 0.77 μm .

One can see that the same number of ions is stopped in a narrower region in the case of Bi irradiation, both in depth and radial direction. In the same time, there is a higher difference in size and mass of Bi ions than of I ones in respect to the Si host atoms, so that the strain induced by Bi ions is more intense, but extended on a more limited region than for I irradiated samples.

In order to show that the utilisation of the SRIM code instead of a code which keeps into account the crystalline structure of the sample, e.g. *Crystal-transport and range of ions in matter* (CTRIM) or MARLOWE is justified, as the 3° tilt angle between the beam direction and the surface normal is higher than the critical angle for channelling for the [100] surface at the energy considered [17], we have simulated the penetration of Bi ions of 28 MeV energy in Si (100), for orientations of the beam in respect to crystal axes characterised by the polar and azimuthal angles ϑ and φ [18] using the Monte Carlo CTRIM code. The main difference is the consideration of a crystalline target in CTRIM instead of an amorphous one in SRIM, and this is also related to the interatomic potential.

A comparison of the results obtained for the distribution of Bi stopped ions using SRIM with those produced using CTRIM and corresponding to different orientations is presented in Fig. 3.

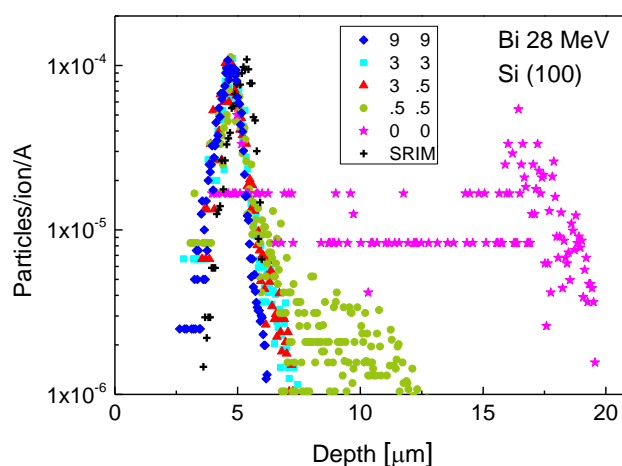


Fig. 3 Comparison between the depths distributions obtained from SRIM and CTRIM for orientations of the beam in respect to (100) characterized by the angles ϑ and φ listed in the legend

It appears that with the exception of the (100) channelling direction and the direction disoriented in respect to it by very small angles of 0.5 and 0.5 $^\circ$ respectively, the distributions are similar, with a peak situated in the region 4.5 - 5 μm , and have similar widths. They are the random

Pearson distributions [19, 20]. On the channelling direction and on the direction close to it, ion penetration is greatly enhanced, as first found by Nelson and Thompson [21] for 75-keV protons through thin crystals of Au. The theory of channelling was shortly developed, with an important contribution by Jens Lindhard [22], which introduced the concept of average or continuum potential. On these two directions, there is a dual Pearson distribution of the stopped ions, which has random and channelled components [19, 20], the contribution of the second one being maximum on the channelling direction.

The difference between ion ranges as a function on the reciprocal orientation ion-crystal can be better understood by plotting the total energy loss as a function of ion penetration into Si. This is illustrated for the case of Bi in Fig. 4. In the inset, the corresponding electronic (full symbols) and nuclear (empty symbols) components are represented as a function of ion penetration depth. So, if the direction of a charged particle incoming upon Si surface lies close to a major crystal direction (i.e. close to a high symmetry axis as (100)), with high probability the particle only suffers a correlated series of small-angle collisions as it passes through several layers of atoms in the crystal and hence remains in the same crystal “channel”. Both electronic and nuclear energy losses are lower in the channel, and the consequence is a higher penetration depth.

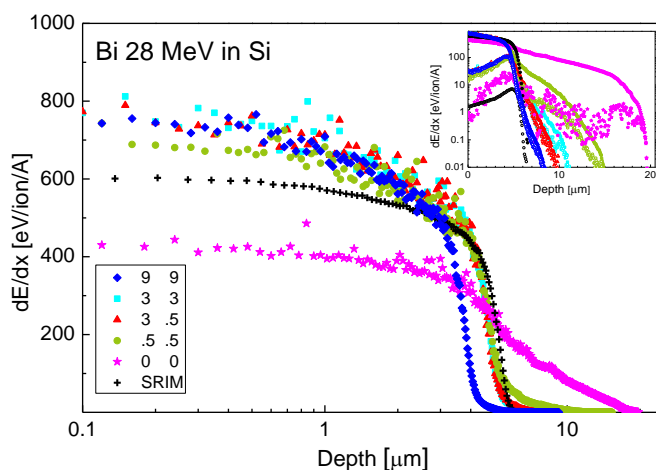


Fig. 4. The energy loss of Bi ions, of initial kinetic energy 28 MeV, in Si for different orientations of the beam in respect to the Si lattice; inset – electronic (full symbols) and nuclear (empty symbols) energy loss dependence on the depth under the surface

2.2 Distribution of primary defects

The depth distributions of the primary defects produced by Bi and I irradiation, as obtained from SRIM simulations, are presented in Figs. 5 and 6 respectively: 3D profile, contour plot in the depth-radius plane, and depth distribution.

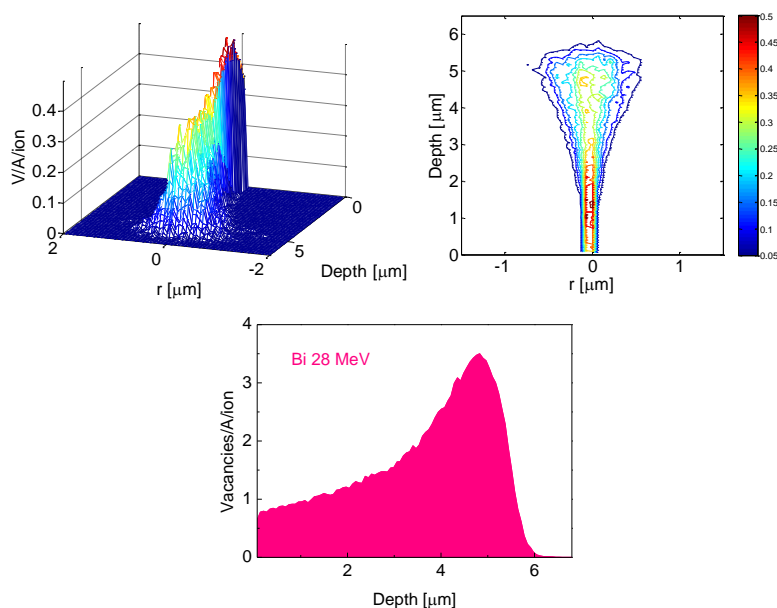


Fig. 5. Distribution of primary defects created in Si by Bi irradiation. From left to right: 3D profile, contour plot in the depth-radius plane, and depth distribution

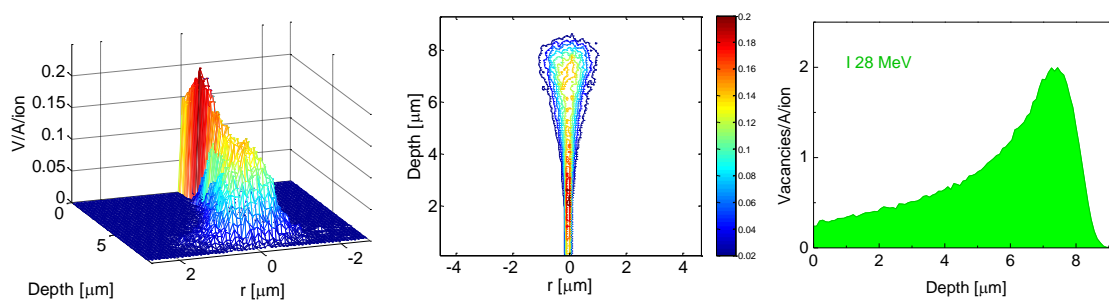


Fig. 6. Distribution of primary defects created in Si by I irradiation. From left to right: 3D profile, contour plot in the depth-radius plane, and depth distribution

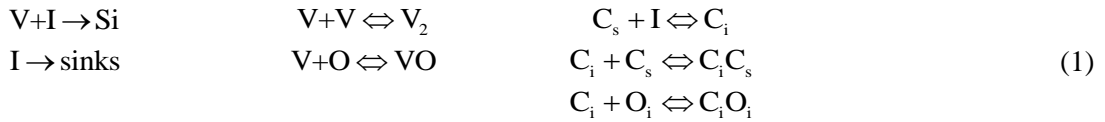
As can be observed, there is an important tail of the vacancy distribution toward the surface, and it is the consequence of the process of slowing down, characterized by the cascade of displacements produced by each incoming ion. At each depth on its range, both the incident ion and all knock-on ions create vacancy – interstitial pairs, the maximum of the distribution being situated near the end of range, where the nuclear stopping has the maximum.

By comparing the distributions of primary defects with the distribution of ions, one can see that for both Bi and I the maximum of vacancy distribution does not coincide with the maximum of the distribution of stopped ions, being situated toward the surface of the sample. Moreover there is an important region under the surface characterized by the presence of primary defects, but without stopped ions.

3. Stable defects and their characterisation

In Si both vacancies and interstitials have a high mobility, and consequently during their migration they interact between themselves [23] annihilating or producing divacancies (V_2), the interstitials migrate to sinks (*e.g.* the surface), and interact also with the other impurities existing in silicon, as O, C and also doping P, thus forming the following defects, stable at room temperature:

vacancy-oxygen (VO), interstitial carbon (C_i), interstitial carbon- interstitial oxygen (C_iO_i), and interstitial carbon-substitutional carbon (C_iC_s), and vacancy-phosphorous (VP). Due to reaction kinetics, C_i , formed by the interaction of a substitutional C atom with an interstitial, is quickly consumed in the formation of C_iO_i and C_iC_s . On the other hand, in our samples of high resistivity there is a low concentration of P, and the concentration of VP can be neglected. So, the main defects expected to form by Bi and I irradiation are: V_2 , C_iO_i and C_iC_s [24]. All of them have energy levels in the band gap [25], and consequently act as traps for the charge carriers. By considering the following reaction kinetics:



with the energies of formation and decomposition of defects from Refs. [26, 27, 28] the distribution of stable defects can be found, starting in each case from the distribution of primary defects represented in Figs. 6 and 7 and taking into account the concentrations of O and C, considered to be uniformly distributed (see Ref. [29]).

In order to find their trapping characteristics, we used the method of thermally stimulated currents without applied bias, which is characterized by a superlinear dependence of the current on the concentration of trapping centres [30-32]. The method is suitable for the characterization of these samples as the concentrations of defects are expected to be relatively low. Moreover, it permits the investigation of defects in the depth of the sample; this is based on defect charging at low temperature by illumination with light of different wavelengths, which has different absorption depths. Thus we chose for our samples three wavelengths, of 1000, 800 and 400 nm [15, 16], which enable charging the traps in all the depth of the sample, in the region up to 10 μm , and in the surface layer [33]. The illumination is made through the irradiated surface, which has a semitransparent metallic contact. After illumination which is long enough to ensure charge trapping, the sample is heated with a low constant rate, and the relaxation current is recorded. Charge carriers are detrapped from the defects, and they move in an internal electric field, as now external field is applied. This field is the superposition of the electric field created by the still trapped charge carriers and an electric field corresponding to the strain introduced by the presence of stopped ions. In fact, an electric field gradient is the effect of the strain existing in the lattice [34], and in the modelling of our relaxation curves we considered an effective electric field, which is the integral of the electric field gradient over the thickness of the sample. While the electric field due to trapped charge carriers is continuously changing in time due to traps discharging during heating, the last one is permanent and temperature independent, and it is expected to be higher in Bi than in I irradiated samples.

By modelling relaxation curves measured on both Bi and I irradiated samples [15, 16], the parameters of the traps (activation energy, concentration and capture cross section) as well as the electric field associated to the field of strain were obtained. This was performed by solving the system of coupled differential equations for the trapped carrier concentrations [35], with trap characteristics and intensity of the electric field corresponding to the strain as parameters.

In the aim of finding the influence of the strain field on the parameters of traps, we modelled separately the discharge curves corresponding to Bi and I irradiation. For each ion, the relaxation curves corresponding to the three mentioned wavelengths illumination were modelled together.

From the experimental curves we found, by modelling, that in both Bi and I irradiation case, the defects V_2 , VO, C_iC_s , C_iO_i are present in the samples. These defects are identified by comparing the energy levels determined by the fitting procedure with those reported in the literature [25].

4. Discussion

The penetration of Bi and I ions of 28 MeV in Si was simulated with SRIM, a Monte Carlo code appropriate for amorphous targets, and we demonstrated that this is justified in the present case, as the critical angle for channelling for this energy is lower than the disorientation between the beam axis and the (100) Si axis. The demonstration was made by using the CTRIM code that considers the crystalline structure of Si, and that gave results close to those from SRIM.

From the analysis of both the simulation of the distribution of stopped Bi and I ions into Si and the simulation of the distribution of primary defects produced during their slowing down, we found that in both cases of Bi and of I there is an important superposition between these regions. As permanent defects are located in nearly the same region as primary ones, all effects investigated are related to this superposition zone, where the strain due to the presence of bigger and heavier ions in respect to Si lattice atoms determines changes in the electrical properties of radiation induced defects. Bi irradiation produces a stronger damage (higher nuclear energy loss and consequently more vacancies/ion) that is more concentrated (lower range) in respect to I irradiation.

The strain produced by Bi ions is also more intense than that produced by I ions, due to the higher difference in atomic mass and size between Bi and Si in respect to I and Si. So, the atomic masses and radii are 209 and 1.70 Å respectively for Bi, 127 and 1.28 Å for I and 28 and 1.17 Å for Si. This difference in strain intensity is reflected in the behaviour of traps. Two main differences between trap parameters in Bi and I irradiated Si samples were evidenced [15, 16]. So, while in Bi irradiated samples all trapping levels are broadened having Gaussian distributions (18-30 meV) and their capture cross sections depend on temperature as $1/T^2$, in I irradiated samples all traps have discrete energy levels and temperature independent capture cross sections. More than that, as it results from modelling of experimental curves [16], the electric field corresponding to the strain produced by the stopped ions is two times more intense in Bi irradiated samples than in I irradiated ones. This is in good agreement with the increase of the atomic mass and radius.

Previously, in multiquantum well structures we evidenced and characterised another type of strain produced by different expansion coefficients of two neighbour layers of different materials of CaF₂ and Si [36]. In this case, the strain relaxes at a given temperature, and consequently it behaves as a spike that can be described by (stressinduced) traps having cross-sections dependent on peak temperature as a Gaussian distribution. It was shown that films containing nanocrystals/quantum dots [37] are also characterised by the presence of internal strains (tensile or compressive) that strongly influence the properties of the films, improving or hindering them [38].

In the case studied in this paper, the strain is produced by the stopped heavy ions and is permanent. We found that the increase of the strain field intensity from that produced by I ions to that produced by Bi ones in irradiated Si with the same number of ions, but more localized for Bi irradiation, leads to observable results, as broadening the energy levels and making the capture cross sections temperature dependent.

5. Conclusions

The behaviour of high resistivity Si samples irradiated with Bi and I ions of the same electric charge (+6), kinetic energy (28 MeV), fluence (5×10^{11} ions/cm²), having the same orientation in respect to (100) Si plane is investigated. Both species of stopped ions, Bi and I, are bigger and heavier than Si host atoms, and therefore produce a local field of strain at the place of their stopping; the fields of strain produced by different ions add together. On the other side, during their penetration in the Si target, the ions produce vacancies and interstitials, which interact between themselves and with the other impurities from the sample, thus forming permanent defects.

The penetration of the ions in Si was simulated, both using the SRIM and CTRIM codes, and we found that for the direction of interest, namely for 3° off orientation in respect to (100) Si axis they produce similar results. The stopped ions are located in a layer under the surface centred

at 5.09 and 7.65 μm for Bi and I respectively, and have a nearly Gaussian distribution. Thus, 95% of them are located between 4.25 and 6.93 μm for Bi, and between 6.45 and 8.75 μm for I. The distribution of primary defects is asymmetrical, with a long tail toward the surface. The regions with stopped ions and with defects are superposed, but under the surface there is a region without stopped ions.

We found that the trapping characteristics of the defects induced by Bi irradiation are strongly modified, as the energy levels are broadened and the capture cross sections are temperature dependent, while this is not observed for I irradiation. We attribute this behaviour to the higher field of strain produced by the presence of Bi ions.

The results obtained are of interest for the community working in the design and manufacturing of microelectronic devices incorporating strain, including those using dopants with high atomic mass and size in respect to Si (*e.g.* Bi), which are characterised by high coherence times, and are thus promising for use in quantum computing and quantum sensing.

Acknowledgements

This work was supported by the Romanian Ministry of National Education through the NIMP Core Programme PN09-450101.

References

- [1] Y. Sun, S.E Thompson, T. Nishida, *Strain Effects in Semiconductors: Theory and Device Applications*, (Springer, New York) 2010.
- [2] C.K. Maiti, S. Chattopadhyay, L.K. Bera, *Strained-Si Heterostructure Field Effect Devices*, CRC Press Taylor & Francis Group, 2007.
- [3] P.G.T. Agopian, J.A. Martino, E. Simoen, C. Claeys, *ECS Transactions* **35**, 145 (2011)
- [4] A.A. Barlian, W.-T. Park, J.R. Mallon Jr, A. Rastegar, B.L. Pruitt, *Proc IEEE Inst Electr Electron Eng.* **97**, 513 (2009).
- [5] M.M.S. Polash, M.S. Alam, *International Conference on Electrical Engineering and Information & Communication Technology (ICEEICT)* 1-5 (2014).
- [6] S.V. Kumar, S. Seenithurai, M.M. Raja, M. Mahendran, *Journal of Electronic Materials* **44**, 3761 (2015)
- [7] J. Cui, C.-Y.Liang, E.A. Paisley, A. Sepulveda, J.F. Ihlefeld, G.P. Carman, C.S. Lynch, *Appl. Phys. Lett.* **107** 092903 (2015)
- [8] T. van Hemert, R J E Huetting, *IEEE Trans. Electron Devices* **60**, 3265 (2013).
- [9] H. Achour, B. Cretu, E. Simoen, J.-M. Routoure, R. Carin, A. Benfdila, M. Aoulaiche, C. Claeys, *Solid-State Electron.* **112**, 1 (2015).
- [10] A. Naugarhiya, S. Dubey, P.N. Kondekar, *Superlattices and Microstructures* **85**, 461 (2015).
- [11] G.W. Morley Chapter 3: Towards spintronic quantum technologies with dopants in silicon, in "Electron Paramagnetic Resonance, Volume 24, 2014, 24, 62-76 RSC Publishing House.
- [12] R. Roldán, A. Castellanos-Gomez, E. Cappelluti, F. Guinea, *J. Phys.: Condens. Matter* **27**, 313201 (2015).
- [13] R. Herring R, M. Norouzpour, K. Saitoh, N. Tanaka, T. Tanji, *Ultramicroscopy* **156**, 37 (2015).
- [14] B. Fluegel, A.V. Mialitsin, D.A. Beaton, J.L. Reno, A. Mascarenhas, *Nat. Commun.* **6**, 7136 (2015).
- [15] S. Lazanu, A. Slav, A.-M. Lepadatu, I. Stavarache, C. Palade, G. Iordache, and M. L. Ciurea, *Appl. Phys. Lett.* **101**, 242106 (2012).
- [16] M.L. Ciurea, S. Lazanu, A. Slav and C. Palade, *EPL* **108**, 36004 (2014).
- [17] V. Raineri, A. Cacciato, F. Benyaich, F. Priolo, E. Rimini, G. Galvagno and S. Capizzi, *Nucl. Instr. Meth. Phys. Res. B* **62**, 331 (1992).
- [18] M. Posselt, *Radiat. Eff. Defects Solids* 130–131, 87 (1994).
- [19] A.F. Tasch, H. Shin, C. Park, J. Alvis, S. Novak, *J. Electrochem. Soc.* **136**, 810 (1989)
- [20] K.M. Klein, C. Park, A. F. Tasch, R.B. Simonton, S. Novak, *J. Electrochem. Soc.*

- 138**, 2102 (1991).
- [21] R. S. Nelson and M. W. Thompson, *Phil. Mag.* **8**, 1677 (1963); erratum: *Phil. Mag.* **9**, 1069 (1964).
- [22] J. Lindhard, K. Dan. Vidensk. Selsk. Mat. -Fys. Medd. **34**, No. 14 (1965).
- [23] S. Lazanu, M.L. Ciurea, I. Lazanu, *J. Optoe. Adv. Mat.* **11**, 2150 (2009).
- [24] M. L. Ciurea, V. Iancu, S. Lazanu, A. M. Lepadatu, E. Rusnac, I. Stavarache, *Rom. Rep. Phys.* **60**, 735 (2008).
- [25] P. Pichler, *Intrinsic point defects, impurities and their diffusion in silicon*, Springer Verlag Wien 2004.
- [26] I. Lazanu, S. Lazanu, *Phys. Scripta* **67**, 388 (2003).
- [27] S. Lazanu, I. Lazanu, *Phys. Scripta* **69**, 376 (2004).
- [28] I. Lazanu, S. Lazanu, *Physica Scripta.* 71, 31 (2005).
- [29] C. Palade, A-M. Lepadatu, A. Slav, M.L. Ciurea, S. Lazanu, private communication
- [30] D. Petre, I. Pintilie, T. Botila, M.L. Ciurea, *J. Appl. Phys.* **76**, 2216 (1994).
- [31] V. Iancu, M.L. Ciurea, M. Draghici, *J. Appl. Phys.* **94**, 216 (2003).
- [32] D.Valentovic, J. Cervenak, S. Luby, M.L. Aldea, T. Botila, *Phys. Status Solidi A* **56**, 341 (1979).
- [33] M. A. Green and M. J. Keevers, *Prog. Photovoltaics* **3**, 189 (1995).
- [34] C Brusewitz, U Vetter and H Hofsass, *J. Phys.: Condens. Matter* **27**, 055401(2015).
- [35] M.L. Ciurea, V. Iancu, M.R. Mitroi, *Solid- State Electron.* **51**, 1328 (2007).
- [36] M.L. Ciurea, *P. Romanian Acad. A* **12**, 315 (2011).
- [37] C. Trisca-Rusu, A. C. Nechifor, S. Mihai, C. Parvu, S. I. Voicu, G. Nechifor, 2009 International Semiconductor Conference (CAS), Sinaia, Romania, 2009, Vol. 1 (IEEE, New York, 2009), pp. 285–288. “Polysulfone-functionalized multiwalled carbon nanotubes composite membranes for potential sensing applications”
- [38] M. Braic, V. Moagar, A. Vladescu, A. Kiss, C. Trisca-Rusu, M. Balaceanu, V. Braic, presented at the International Workshop on Nanostructured Materials, June 21-23 -th, 2006, Antalya, Turkey.